Biophysical Reports

REPORT

Is orange carotenoid protein photoactivation a single-photon process?

Stanisław Niziński,[1,2,*] Ilme Schlichting,[3] Jacques-Philippe Colletier,[4] Diana Kirilovsky,[5] Gotard Burdzinski,[1,*] and Michel Sliwa[2,*]

[1]Quantum Electronics Laboratory, Faculty of Physics, Adam Mickiewicz University in Poznań, Poznan, Poland; [2]Univ. Lille, CNRS, UMR 8516 - LASIRE, Laboratoire Avancé de Spectroscopie pour les Interactions, la Réactivité et l'Environnement, Lille, France; [3]Max-Planck-Institut für medizinische Forschung, Heidelberg, Germany; [4]Université Grenoble Alpes, CEA, CNRS, Institut de Biologie Structurale, Grenoble, France; and [5]Université Paris-Saclay, CEA, CNRS, Institute for Integrative Biology of the Cell (I2BC), Gif-sur-Yvette, France

ABSTRACT In all published photoactivation mechanisms of orange carotenoid protein (OCP), absorption of a single photon by the orange dark state starts a cascade of red-shifted OCP ground-state intermediates that subsequently decay within hundreds of milliseconds, resulting in the formation of the final red form OCP^R, which is the biologically active form that plays a key role in cyanobacteria photoprotection. A major challenge in deducing the photoactivation mechanism is to create a uniform description explaining both single-pulse excitation experiments, involving single-photon absorption, and continuous light irradiation experiments, where the red-shifted OCP intermediate species may undergo re-excitation. We thus investigated photoactivation of *Synechocystis* OCP using stationary irradiation light with a biologically relevant photon flux density coupled with nanosecond laser pulse excitation. The kinetics of photoactivation upon continuous and nanosecond pulse irradiation light show that the OCP^R formation quantum yield increases with photon flux density; thus, a simple single-photon model cannot describe the data recorded for OCP *in vitro*. The results strongly suggest a consecutive absorption of two photons involving a red intermediate with ≈100 millisecond lifetime. This intermediate is required in the photoactivation mechanism and formation of the red active form OCP^R.

WHY IT MATTERS We question whether the $OCP^O \rightarrow OCP^R$ photoconversion can be completed upon absorption of only a single photon, as implicitly assumed in the literature. This quest is important from a biological point of view, as one can expect that the photoactivation mechanism of OCP should be as selective as possible. The proposed two-photon mechanism fulfills this condition perfectly because it allows efficient OCP photoactivation (and quenching excited phycobilisomes) above a light threshold of around 1 mW/cm^2 (≈ 40 $\mu mol\ m^{-2}\ s^{-1}$) but not at low light conditions, where any dissipative mechanism is very unfavorable, because it would reduce photosynthesis efficiency. One should expect a clear evolutionary advantage for cyanobacteria possessing such a two-photon photoprotective mechanism compared with much less selective single-photon mechanism.

INTRODUCTION

Orange carotenoid protein (OCP) (1) is a photoactive protein, acting as a photoprotective factor in cyanobacteria (2,3). The dark-adapted form (OCP^O due to its orange color) can be photoconverted into the active form (OCP^R due to red-shifted absorption spectrum) by blue or green light. OCP^R is capable of quenching excited phycobilisomes (PBSs), protecting reaction centers from energy overload, thus avoiding formation of reactive oxygen species (4). The photoconversion process $OCP^O \rightarrow OCP^R$ starts with absorption of a photon, which triggers hydrogen bond cleavage enabling carotenoid translocation into the N-terminal domain (NTD) (5,6), followed by NTD and C-terminal domain separation on the millisecond timescale (7–9).

The majority of the recent models of OCP photoconversion have been proposed based on the *in vitro* evolution of absorbance induced by a laser pulse excitation spanning temporal regimes from hundreds of femtoseconds to single seconds (5,8,10,11). These

Submitted April 18, 2022, and accepted for publication August 17, 2022.

*Correspondence: nizin@amu.edu.pl or gotardb@amu.edu.pl or michel.sliwa@univ-lille.fr

Twitter: @michelsliwa

Editor: Hagen Hofmann.

https://doi.org/10.1016/j.bpr.2022.100072

techniques are very powerful in tracking short living species, but they have also a major drawback: the observation of the final OCP^R state is very challenging due to a very low formation quantum yield. When seeking biologically relevant information, continuous irradiation is superior to pulse excitation. Experiments with continuous irradiation reflect the biological conditions very well and allow OCP^R to accumulate, overcoming its ultra-low quantum yield (below 0.2%) (8).

Rakhimberdieva et al. (12) studied light-induced fluorescence changes of the PBSs in a PSII-deficient mutant of *Synechocystis*. They measured action spectrum, which is magnitude of fluorescence quenching represented in function of wavelength of irradiation light used to induce the quenching (while keeping fixed fluorescence excitation light at 580 nm). 10 s irradiation was used with photon flux density above 200 μmol m^{-2} s^{-1}. This spectrum has been found to overlap with dark-adapted OCP absorption spectrum (13).

Wilson et al. (3) presented how temperature and irradiation intensity affect the photoactivation speed. They investigated the mechanism of non-photochemical quenching tracking PBS fluorescence *in vivo* and the photoconversion OCP from *Synechocystis* containing hydroxyechinenone using absorption spectroscopy *in vitro*. They used spectrally broad irradiation light in the band from 400 to 550 nm with irradiances between 20 μmol m^{-2} s^{-1} and 1.2 mmol m^{-2} s^{-1}. The most important conclusion was that low temperature and high light intensity facilitate efficient formation of quenching-capable OCP^R. They found that the initial slope of the photoactivation kinetics (dA/dt) correlates with the irradiation intensity and the quantum yield of photoactivation is about 1% when using femtosecond transient absorption spectroscopy. Moreover, variation of the temperature (11°C–32°C) did not affect the initial dA/dt (3).

Gorbunow et al. (14) investigated *in vivo* the quenching of PBS fluorescence with wild-type OCP from *Synechocystis* (and other strains). The OCP photoactivation was triggered by 470 nm light, with various photon flux densities from 10 μmol m^{-2} s^{-1} to 15 mmol m^{-2} s^{-1}. In agreement with Gwizdala et al. (15) and Rakhimberdieva et al. (16), they introduced a three-state model containing an additional non-quenching intermediate (7 s lifetime) before the formation of quenching centers and determined the quantum yield *in vivo* to be 0.1% (14).

The first model for the *in vitro* photoconversion of purified OCP was proposed by Maksimov et al. (17). They measured the kinetics of the absorbance at 550 nm upon 460 nm irradiation (photon flux density up to 4 mmol m^{-2} s^{-1}, only one experiment below 200 μmol m^{-2} s^{-1}), using OCP from *Arthrospira maxima* with the hydroxyechinenone chromophore. They concluded that the rate of photoactivation grows linearly with light intensity (17). They also applied the same three-states scheme proposed for OCP *in vivo*. In purified OCP, the non-quenching intermediate was found to live below instrument resolution (0.1 s) (17). They found that the photoactivation quantum yield is about 0.1%, just like the formation quantum yield of quenching centers *in vivo*. Maksimov et al. (17) reported two more important observations: firstly, the OCP^R decay is not monoexponential, and secondly, its lifetime in the dark depends on the applied photon flux density.

In the following report, Maksimov et al. (9) performed a transient absorption experiment *in vitro* with 532 nm nanosecond pulse excitation in the μs to second temporal range, using N-tagged OCP from *Synechocystis*. They calculated the quantum yield of OCP^R formation to be around 0.2%. A red intermediate OCP^{RI} living around 0.3 ms (at 36 °C) was observed and identified as a precursor of the final long-lived photoactive OCP^R.

In the latest report, Maksimov et al. (8) used a mutant protein that contained only one tryptophan (Trp-288), which forms an H-bond with the carotenoid, to track cleavage of this bond following illumination using tryptophan fluorescence measurements. Using 5 ms and 100 ms flashes of 450 nm light, they found additional intermediate states in the millisecond timescale before the formation of active OCP^R: P_N (τ = 10 ms), P_M (τ = 35 ms), and P_X (τ = 100 ms) at 20°C. The $P_X \rightarrow OCP_R$ process was assigned to C-terminal domain and NTD separation.

Recently, Mezetti et al. identified an interesting two-step evolution in the seconds timescale upon continuous irradiation using Fourier transform infrared probing (at 4 °C), both associated with α-helix reorganization (18).

Thus, the literature about formation of the active form OCP^R is already quite rich. However, several incoherent perspectives exist. Moreover, the studies done so far explored mostly the high intensity irradiation regime, whereas the *in vivo* biological working conditions of OCP are limited by the light intensity of the sun. The total photon flux density of the sun in the 420 to 550 nm wavelength range (which is the OCP sensitivity region) is below 1000 μmol m^{-2} s^{-1} (solar photosynthetic photon flux density equals 2200 μmol m^{-2} s^{-1} for noon at the equator at equinox (19)). Therefore, light intensities exceeding this range do not represent the conditions naturally encountered by the OCP *in vivo*. In fact, OCP should already perform its photoprotective function efficiently much below these light levels, because 1) in most places on Earth, the solar intensity is much weaker than at the equator, 2) usually OCP is not directly exposed to sunlight as it is confined

in cyanobacteria cells, 3) the water surface will reflect part of the incident light, etc.

For all these reasons, we investigate here the photoactivation in the lower irradiation intensity regime of the most studied *Synechocystis* OCP containing the ECN chromophore (echinenone). We used C-tagged and N-tagged OCP variants for which we have reported recently diametrically different photoactivation speeds (20). To ensure that our results reflect the natural working conditions of OCP, we limited our photon flux density range to about 200 μmol m^{-2} s^{-1}, which certainly does not exceed the biological photoexcitation regime of OCP *in vivo*. We designed a nanosecond transient absorption experiment combined with continuous irradiation to investigate the re-excitation of millisecond lifetime intermediates that could participate in the photoactivation process. Our experiment revealed that upon additional continuous irradiation, the laser pulse-induced ΔA signal dramatically increases, which eliminates the hypothesis that OCP^R formation is purely a single-photon process.

Efficiency of the photoactivation: Is the single-photon mechanism valid?

To begin with, we investigated photoactivation using stationary absorption spectroscopy as a function of irradiation photon flux density, with probing done at the OCP^R absorption band (Fig. S1 *a*). Fig. 1 shows the difference absorbance (subtraction of absorbance at time zero; see supporting methods in the supporting material) induced by 452 nm irradiation, probed at 580 nm for C-tagged OCP. A comparison between the N-tagged and C-tagged protein is presented in the supporting material (Fig. S2). In order to quantify the efficiency of photoactivation, one can calculate the derivative dA/dt during the first seconds of irradiation, where the growth of the absorbance is still linear (using linear fits, presented in Fig. S3). The dA/dt value obtained this way is plotted in Fig. 2 *a*, and it represents the speed of photoactivation. If the process is caused by absorption of a single photon, one would expect that doubling the irradiation intensity should result in a doubled rate of OCP^R accumulation (so dA/dt should also double). This can be visualized in a log-log plot, where this dependence should result in a linear fit with slope equal to 1. Linear fits in Fig. 2 *a* (*dashed line*) show that both C-tagged and N-tagged OCPs are characterized by a slope higher than 1 (meaning that doubling light intensity causes more than doubled speed of photoactivation), with a larger slope determined for C-tagged OCP. The C-tagged dataset was measured twice, with 550 (green) and 580 nm (red) probing, to ensure that the slope value is reproducible.

Before going further, it is required that we define the quantum yield of OCP photoactivation, i.e., the quantum yield of OCP^R formation for a simple photochemical one-photon process (pictured in Fig. 2 *c*). It can be formulated as a reaction rate equation (21):

$$\frac{d\left[OCP^R\right]}{dt} = \varphi\, I_0\, F\, \left[OCP^O\right] \epsilon_{OCP^O}\, l_{irr} - k_{OCP^R \rightarrow OCP^O} \left[OCP^R\right] \quad (1)$$

$$F = \left(1 - 10^{-A_{irr}}\right)/A_{irr}, \quad (2)$$

where φ is the quantum yield of OCP^R formation using 452 nm irradiation wavelength. It assumes that all thermal processes occurring after photon absorption lead back to the initial OCP^O state or generate the OCP^R with a probability equal to φ. So, the φ term should be understood as a "black box" that encapsulates various relaxation schemes initialized by absorption of the single photon. F is the so-called photokinetic factor. A_{irr} is the total absorbance of the sample solution at irradiation wavelength and optical path length (l_{irr}). $[OCP^O]$ and $[OCP^R]$ are molar concentrations of OCP^O and OCP^R, respectively. I_0 is the photon flux density measured in moles of photons s^{-1} L^{-1}. $k_{OCP^R \rightarrow OCP^O}$ is associated with the thermal back recovery, i.e., the inverse of the OCP^R decay time constant ($\tau_{OCP^R \rightarrow OCP^O}$; k in Fig. 2 *c*). ϵ_{OCP^O} is the molar absorption coefficient of OCP^O at irradiation wavelength (452 nm).

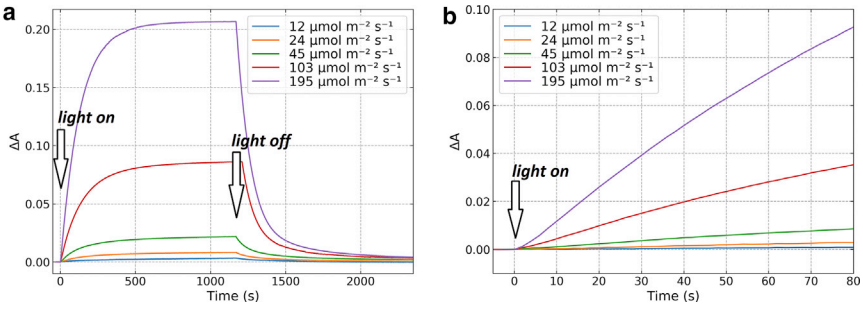

FIGURE 1 (*a*) Difference absorbance kinetics recorded at 580 nm of C-tagged OCP recorded upon 452 nm irradiation. (*b*) Zoom in at the initial rate of photoactivation. To obtain the light intensity in mW cm^{-2}, multiply the value given in μmol m^{-2} s^{-1} by a factor of 0.026.

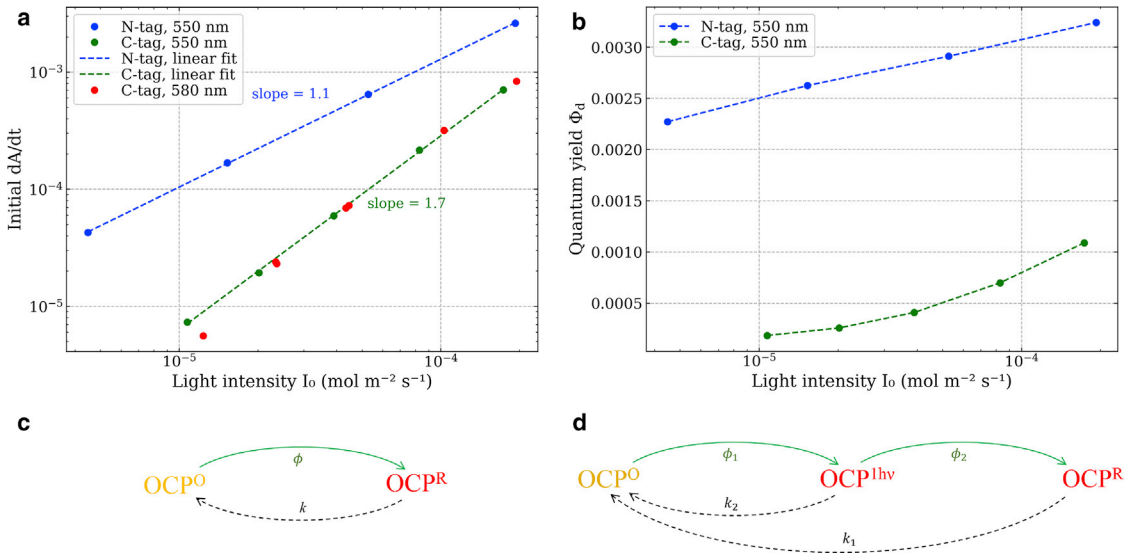

FIGURE 2 (*a*) Initial photoactivation speed dA/dt plotted versus light intensity using log-log graph. (*b*) Differential photoactivation quantum yield formation of OCP^R calculated using Eq. 3 for N-tagged and C-tagged OCPs. (*c*) Single-photon model. (*d*) Example of a two-photon model.

$k_{OCP^R \rightarrow OCP^O}\,[OCP^R]$ term can be understood as decrease in OCP^R concentration per second due to thermal relaxation. $[OCP^O]\,\epsilon_{OCP^O}\,l_{irr}$ represents the absorbance of all OCP^O species, which, when multiplied by F, becomes the probability that a photon of irradiation light is absorbed by the OCP^O species in the sample solution (but not by OCP^R). Going further, this probability multiplied by $\varphi\, I_0$ is linked to the decrease of OCP^O concentration per second, caused by photoconversion of OCP^O into OCP^R. Therefore, overall $d[OCP^R]/dt$ originates from species being photoactivated to OCP^R minus species relaxing back to the OCP^O state.

From Eq. 1, it is clear that in the initial period of the irradiation (much shorter than OCP^R thermal back recovery time constant,), the OCP^R concentration should indeed grow linearly with time. Only when the irradiation timescale approaches $\tau_{OCP^R \rightarrow OCP^O}$ the concentration profile will start to flatten, settling finally in the photostationary state (in which concentrations of OCP^R and OCP^O do not change anymore). Since the OCP^R lifetime is long, in the order of single minutes (Table S1, at room temperature), one can fit the initial seconds of the evolution of the absorbance during irradiation to extract the OCP^R formation quantum yield φ (Fig. S3). At the early stages of irradiation, the depletion of the dark OCP^O state is negligible, and OCP^R is too weakly populated to allow its decay to play any role, so the kinetics can be approximated by a straight line. Note, it has been demonstrated that there is no light-induced back conversion, the $OCP^R + h\nu \rightarrow OCP^O$ pathway is then blocked (3). By neglecting thermal back recovery in Eq. 1, one can obtain a simplified expression and determine the quantum yield of OCP^R formation from initial dA/dt value:

$$\varphi_d = \frac{dA_{probe}}{dt}\,\frac{1}{I_0\, I_{probe}\, \Delta\epsilon_{OCP^R}\, F_{t=0}\, A_{irr,t=0}}. \qquad (3)$$

φ_d is equivalent to a differential quantum yield, defined by IUPAC (22). $\Delta\epsilon_{OCP^R}$ is the OCP^R difference molar absorption coefficient at the probe wavelength ($\epsilon_{OCP^R} - \epsilon_{OCP^O}$; see Fig. S1 *b*). $F_{t=0}\, A_{irr,t=0}$ is the photokinetic factor multiplied by the absorbance of the solution at the irradiation wavelength, at the $t = 0$ time point, when the irradiation light was just switched on. One can obtain Eq. 3 directly from the Eq. 1, using the Beer-Lambert law and substituting molar concentrations. Differential quantum yields of OCP^R formation calculated this way are presented in Fig. 2 *a*.

The results obtained this way are quite unexpected. One can clearly see in Fig. 2 *b* that for experiments performed with a higher irradiation intensity, one obtains a much higher differential quantum yield φ_d. Therefore, it is clear that a single-photon mechanism for the formation of OCP^R (pictured in Fig. 2 *c*) cannot describe the data (the photoactivation quantum yield φ_d should be the same regardless of the irradiation power, which stems from Eq. 1). It is especially striking for C-tagged OCP, where the differential quantum yield increases more than fourfold in the range of used irradiation intensities (Fig. 2 *b*). The obvious inherent contradiction that the quantum yield Φ in a single-photon model must be constant for any light intensity rules out not only the simple $OCP^O + h\nu \rightarrow OCP^R$ model but in fact any model where absorption of a single

photon starts a cascade of intermediates leading to OCP^R. An additional justification of our conclusion is shown in the supporting material, where we present simulated differential quantum yields (Fig. S4) using exemplary single-photon (Φ, Fig. 2 *c*) and two-photon models (Φ_1 x Φ_2, Fig. 2 *d*; see detailed description in supporting material). The curvature observed in Fig. 2 *b* can only be reproduced with a two-photon model (Fig. S4).

Decay absorption kinetics after nanosecond laser pulse excitation are affected by the intensity of auxiliary continuous light

To further solidify our results on the existence of two-photon pathway for the formation of OCP^R, influence of continuous irradiation on laser pulse-induced transient absorption kinetics of OCP was investigated. Red traces in Fig. 3 show the ΔA evolution at 550 nm after a 532 nm nanosecond laser pulse, without additional continuous irradiation. A red-shifted species with roughly one hundred millisecond lifetime is observed (180 ms for C-tagged OCP and 100 ms for N-tagged OCP). According to literature, this time constant could be associated with the decay of P_X species and domain separation process (8). In C-tagged OCP, the signal recorded after 1 s decays almost to zero ($\Delta A(1\ s) \approx 2.5 \times 10^{-5}$; Fig. 3 *a*, *red trace*). It shows that the single-photon channel leading to photoactivated OCP^R is negligible for C-tagged OCP.

In order to directly observe how two-photon process influences the formation of OCP^R, additional 452 nm continuous irradiation with various intensities was applied (see the supporting material for a detailed description of the experimental setup). ΔA represents increase of absorption signal after the ns laser pulse, compared with the reference measurement where no laser pulse is present. Additional continuous irradiation is applied during both laser-pulse and reference cycles. At high continuous irradiation intensity (Fig. 3 *b*, *cyan curve*), some fraction of OCP will be photoconverted to the OCP^R state, reducing the number of available OCP^Os that can contribute to the laser pulse-induced signal. Therefore, additional continuous irradiation should decrease the $\Delta A(t)$ signal unless some type of interplay between both continuous and laser pulse light is present.

If formation of a single OCP^R protein requires absorption of two consecutive photons (like in Fig. 2 *d*), then application of continuous light irradiation generates a steady-state population of intermediate states (denoted as $OCP^{1h\nu}$; Fig. 2 *d*) that can be subsequently transformed into OCP^R after absorption of a second photon (delivered by ns laser pulse), effectively increasing ΔA signal at 1 s. If OCP photoactivation is triggered by a single-photon absorption, then no such effect should be observed.

Fig. 3 shows clearly that red-shifted species are populated more efficiently in the presence of additional continuous light. Indeed, both N-tagged and C-tagged OCPs exhibit increased ΔA at 1 s (OCP^R concentration) at 550 nm when additional LED irradiation is applied (ΔA at 1 s increases from 2.5×10^{-5} to 3.25×10^{-4} for C-tagged and from 2×10^{-4} to 6.25×10^{-4} for N-tagged OCP; see Fig. 3). This indicates that significant two-photon pathways must be present for both investigated OCPs.

For N-tagged OCP, a single-photon pathway leading to OCP^R cannot be excluded completely due to a positive signal when no continuous irradiation is present (Fig. 3 *b*, *red curve*). However, for C-tagged OCP, the one-photon channel seems to be almost completely blocked, so only the two-photon pathway is allowed to reach OCP^R. One can wonder whether a weak (but still significant) 550 nm probe light could generate enough of the intermediate $OCP^{1h\nu}$ population to enable a sequential two-photon mechanism in N-tagged OCP. Nevertheless, it is evident that N-tagged OCP possesses a very efficient two-photon channel: even a very small amount of external continuous light doubles the signal at 1 s, from 0.2 mOD to 0.4 mOD (Fig. 3 *b*, compare *red* and *orange kinetics*). All these observations are direct evidence that both N-tagged and C-tagged OCPs possess a dominant two-photon photoactivation channel.

One remark should be made on the continuous irradiation: it generates not only a stationary population of

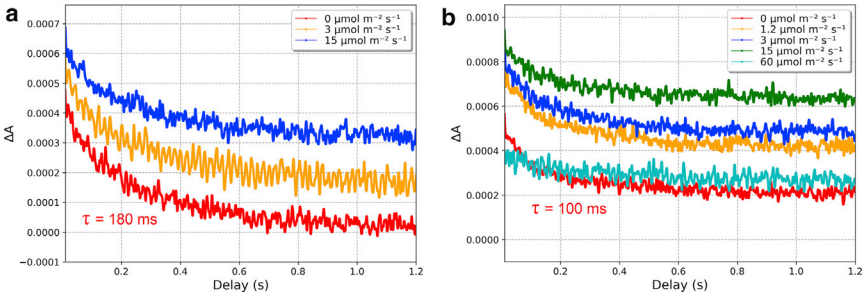

FIGURE 3 (*a* and *b*) Nanosecond laser pulse-induced ΔA kinetics (5 mJ, 532 nm) probed at 550 nm in the presence of various intensities of stationary LED irradiation at 452 nm for (*a*) C-tagged and (*b*) N-tagged OCP. The indicated time constant was retrieved using a monoexponential fit of the red curve (no 452 nm LED irradiation).

the $OCP^{1h\nu}$ intermediate states but also OCP^R at a much larger number. Therefore, at some threshold intensity of continuous irradiation light, ΔA should not increase anymore due to a significant depletion of the dark-adapted OCP^O form. If most of the sample is photoconverted to OCP^R population by the continuous irradiation, the amplitude of ns pulse-induced ΔA signal should decrease. Note that it was demonstrated that OCP^R is a non-photoactive state (3). Indeed, in N-tagged OCP above 15 μmol m^{-2} s^{-1} light intensity, the signal saturates (Fig. 3 *b*, *green kinetic*), and above 60 μmol m^{-2} s^{-1} intensity, the signal drops significantly (Fig. 3 *b*, *cyan kinetic* at 1 s). As expected, only low levels of continuous irradiation allow us to observe two-photon behavior manifested by an increase in ΔA(1 s) because strong irradiation causes significant depletion of OCP^O.

DISCUSSION

Continuous irradiation experiments and nanosecond pulse with continuous irradiation experiments were performed to bridge photoexcitation with laser pulses and continuous light. A sequential two-photon mechanism is feasible for the continuous LED source above certain power threshold, leading to a differential quantum yield φ_d dependence extracted from the irradiation kinetics (Fig. 2 *b*). Fig. 4 attempts to illustrate this effect by showing a millisecond transient absorption signal obtained after nanosecond excitation superimposed with the integrated number of photons to be absorbed by a single $OCP^{1h\nu}$ molecule living during a given period (which equals $I_0\, F\, \epsilon_{OCP^R}\, l_{irr}\, t$, calculated by integration of Eq. 1). As one can see, this number is close to one photon absorbed within 1 s when 200 μmol m^{-2} s^{-1} light is present. The green area between both curves indicates a temporal region where the probability of absorption of a second photon is significant, and there still exist some intermediate $OCP^{1h\nu}$ states that can absorb another photon. This region is almost negligible for a low light intensity illumination (10 μmol m^{-2} s^{-1}; Fig. 4, *below blue line*) but quite significant for high light intensity (200 μmol m^{-2} s^{-1}; Fig. 4, *below red line*).

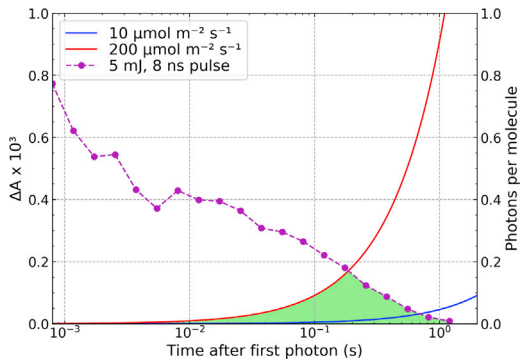

FIGURE 4 ΔA kinetics at 550 nm obtained for C-tagged OCP at 21°C using a nanosecond laser pulse (*red curve* from Fig. 3 *a*) compared with the cumulative number of photons absorbed by $OCP^{1h\nu}$ red intermediate until a given time. For 200 μmol m^{-2} s^{-1} continuous irradiation, the red intermediate formed upon absorption of a single photon and living exactly 1 s will absorb almost 1 photon (which will be its second) on average.

Fig. 4 shows clearly that absorption of a second photon in less than 10 ms after absorption of the first one is very improbable when using biologically relevant light intensities. Therefore, the $OCP^{1h\nu}$ intermediate must live longer than that, otherwise we would not have observed the two-photon absorption characteristics (Fig. 2). One can also exclude that the intermediate lives longer than 1 s because the absorption kinetics grow instantly after switching the light on and ΔA decays instantly after switching the light off (Fig. 1). Therefore, the $OCP^{1h\nu}$ intermediate must be a short-lived state, otherwise one would see an increase in dA/dt (acceleration) at the beginning of the irradiation due to accumulation of the intermediate, which clearly is not the case. The observed ≈100 ms lifetime red-shifted species seems to be a good candidate for $OCP^{1h\nu}$. It seems to be equivalent of P_X state proposed by Maksimov et al. (8) Indeed, the simulation presented in Fig. S4 with the two-photon photochemical scheme of Fig. 2 *d* can reproduce the curvature observed in Fig. 2 *b*. However, it remains an open question whether the decay at 550 nm observed after laser pulse excitation only is really associated with $OCP^{1h\nu}$.

Our results are contradictory to some of the previous reports (3,17) that have concluded a linear dependence of the photon flux density on the initial light-induced dA/dt. However, in previous nanosecond and femtosecond time-revolved absorption experiments, it was shown that only very small fraction of red-shifted OCP species is formed at 1 ns (values between 0.2% and 1.5% are given (5,20)), and almost nothing remains after 1 s (5,7–9,23). We found for C-tagged OCP that upon nanosecond pulse excitation at 532 nm, the absorbance at 550 nm drops to almost zero before 1 s (Fig. 4), indicating that there should not be any long-lived OCP^R species. So, the question arises:how is it possible that upon continuous irradiation, a significant population of OCP^R is formed with a lifetime much longer than 1 s when we clearly see that this species decays much earlier (<1 s) in laser pulse excitation experiments (Fig. 4)? This question leads to the conclusion that a second photon must be required in the mechanism to transform the partially photoactivated "OCP^R-like" ($OCP^{1h\nu}$ from Fig. 2 *d*) intermediate into a long-living OCP^R red form. If a sequential two-photon mechanism is indeed present, then discrepancies between this and various previous studies

may originate from different repetition rates of the experiments. With repetition rates faster than 1 Hz, it is also possible that the observed species are a result of absorption of two consecutive photons (or more). For example, in our nanosecond experiments, we have found that the ΔA kinetics depend on the repetition rate; the usage of a single laser pump pulse per 10–20 s was required to avoid this effect.

CONCLUSIONS

Here, we present compelling evidence that the mechanism of OCP photoactivation cannot be described by single-photon absorption, followed by a chain of thermally decaying intermediates leading to the OCP^R, as described in the currently available literature. We found that absorption of a second photon must be incorporated into the photoactivation mechanism. From our data, it is also clear that the location of His-tag (facilitating protein purification) affects the millisecond kinetics and nature of the photoactivation in a dramatic way, resulting in different photoactivation speeds (20). In C-tagged OCP, the two-photon nature is much more pronounced compared with N-tagged OCP. Nevertheless, the nanosecond laser pulse-induced kinetics points to a two-photon photoactivation mechanism also in N-tagged OCP because the ΔA signal at 1 s triples upon auxiliary continuous irradiation (0.002 to 0.006; Fig. 3 *b*). In C-tagged OCP, our data exclude a single-photon photoactivation channel because almost no ΔA signal is observed at 1 s after nanosecond pulse excitation. The majority of the photoactivation models proposed so far for OCP take the form of different $OCP^O \rightarrow P_1 \rightarrow P_2 \rightarrow \ldots \rightarrow OCP^R$ chains (5,8). We believe that this commonly accepted single-photon mechanism must be reevaluated.

SUPPORTING MATERIAL

Supporting material can be found online at https://doi.org/10.1016/j.bpr.2022.100072.

AUTHOR CONTRIBUTIONS

Conceptualization, S.N., M.S., G.B., D.K., and J.-P.C.; methodology, S.N., M.S., G.B., D.K., and J.-P.C.; simulations, S.N.; experiments and data analysis, S.N.; resources, D.K.; writing, S.N., M.S., G.B., D.K., and I.S.; supervision, M.S., G.B., D.K., J.-P.C., and I.S.

ACKNOWLEDGMENTS

We are grateful to Adjéle Wilson for supplying the purified proteins. This work was performed with financial support from the Polish National Science Centre (NCN), project 2018/31/N/ST4/03983, and the French National Research Agency (grant ANR-18-CE11-0005).

DECLARATION OF INTERESTS

The authors declare no competing interests.

REFERENCES

1. Kay Holt, T., and D. W. Krogmann. 1981. A carotenoid-protein from cyanobacteria. *Biochim. Biophys. Acta Bioenerg.* 637: 408–414.
2. Wilson, A., G. Ajlani, …, D. Kirilovsky. 2006. A soluble carotenoid protein involved in phycobilisome-related energy dissipation in cyanobacteria. *Plant Cell.* 18:992–1007.
3. Wilson, A., C. Punginelli, …, D. Kirilovsky. 2008. A photoactive carotenoid protein acting as light intensity sensor. *Proc. Natl. Acad. Sci. USA.* 105:12075–12080.
4. Kirilovsky, D., and C. A. Kerfeld. 2016. Cyanobacterial photoprotection by the orange carotenoid protein. *Native Plants.* 2:16180–16197.
5. Konold, P. E., I. H. M. van Stokkum, and J. T. M. Kennis. 2019. Photoactivation mechanism, timing of protein secondary structure dynamics and carotenoid translocation in the Orange Carotenoid Protein. *J. Am. Chem. Soc.* 141:520–530.
6. Leverenz, R. L., M. Sutter, and C. A. Kerfeld. 2015. A 12 Å carotenoid translocation in a photoswitch associated with cyanobacterial photoprotection. *Science.* 348:1463–1466.
7. Wilson, A., E. A. Andreeva, J. P. Colletier…, 2022. Structure-function-dynamics relationships in the peculiar Planktothrix PCC7805 OCP1: impact of his-tagging and carotenoid type. *Biochim Biophys Acta Bioenerg.* 1863 (7):148584–148608. https://doi.org/10.1016/j.bbabio.2022.148584.
8. Maksimov, E. G., E. A. Protasova, …, T. Friedrich. 2020. Probing of carotenoid-tryptophan hydrogen bonding dynamics in the single-tryptophan photoactive Orange Carotenoid Protein. *Sci. Rep.* 10. 11729-12.
9. Maksimov, E. G., N. N. Sluchanko, …, A. B. Rubin. 2017. The photocycle of orange carotenoid protein conceals distinct intermediates and asynchronous changes in the carotenoid and protein components. *Sci. Rep.* 7. 15548-12.
10. Yaroshevich, I. A., E. G. Maksimov, …, M. P. Kirpichnikov. 2021. Role of hydrogen bond alternation and charge transfer states in photoactivation of the Orange Carotenoid Protein. *Commun. Biol.* 4:539-13.
11. Kuznetsova, V., M. A. Dominguez-Martin, …, T. Polívka. 2020. Comparative ultrafast spectroscopy and structural analysis of OCP1 and OCP2 from Tolypothrix. *Biochim. Biophys. Acta Bioenerg.* 1861. 148120-11.
12. Rakhimberdieva, M. G., I. N. Stadnichuk, …, N. V. Karapetyan. 2004. Carotenoid-induced quenching of the phycobilisome fluorescence in photosystem II-deficient mutant of Synechocystis sp. *FEBS Lett.* 574:85–88.
13. Karapetyan, N. V. 2007. Non-photochemical quenching of fluorescence in cyanobacteria. *Biochemistry.* 72:1127–1135.
14. Gorbunov, M. Y., F. I. Kuzminov, …, P. G. Falkowski. 2011. A kinetic model of non-photochemical quenching in cyanobacteria. *Biochim. Biophys. Acta.* 1807:1591–1599.
15. Gwizdala, M., A. Wilson, and D. Kirilovsky. 2011. In vitro reconstitution of the cyanobacterial photoprotective mechanism mediated by the Orange Carotenoid Protein in Synechocystis PCC 6803. *Plant Cell.* 23:2631–2643.
16. Rakhimberdieva, M. G., F. I. Kuzminov, …, N. V. Karapetyan. 2011. Synechocystis sp. PCC 6803 mutant lacking both photosystems exhibits strong carotenoid-induced quenching of phycobilisome fluorescence. *FEBS Lett.* 585:585–589.
17. Maksimov, E. G., E. A. Shirshin, …, A. B. Rubin. 2015. The signaling state of Orange Carotenoid Protein. *Biophys. J.* 109:595–607.

18. Mezzetti, A., M. Alexandre, …, D. Kirilovsky. 2019. Two-step structural changes in Orange Carotenoid Protein photoactivation revealed by Time-Resolved Fourier Transform Infrared Spectroscopy. *J. Phys. Chem. B.* 123:3259–3266.

19. Ritchie, R. J. 2010. Modelling photosynthetic photon flux density and maximum potential gross photosynthesis. *Photosynthetica.* 48:596–609.

20. Nizinski, S., A. Wilson, …, M. Sliwa. 2022. A unifying perspective of the ultrafast photo-dynamics of Orange Carotenoid Protein from Synechocystis: peril of high-power excitation, existence of different S* states and influence of tagging. *JACS Au.* 2:1084–1095. https://doi.org/10.1021/jacsau.1c00472.

21. Deniel, M. H., D. Lavabre, and J. C. Micheau. 2002. Photokinetics under continuous irradiation. *In* Organic photochromic and thermochromic compounds volume 2: physicochemical studies, biological applications, and thermochromism. J. C. Crano and R. J. Guglielmetti, eds. Kluwer Academic Publishers, pp. 167–182.

22. Chalk, S. J. 2019. *In* IUPAC. Compendium of Chemical Terminology, Second edition the "Gold Book". https://goldbook.iupac.org/terms/view/Q04991.

23. Andreeva, E. A., S. Nizinski, J. P. Colletier…, 2022. Oligomerization processes limit photoactivation and recovery of the Orange Carotenoid Protein. *Biophys. J.* 121:2849–2872. https://doi.org/10.1016/j.bpj.2022.07.004.